CARBON letters

Note

Carbon Letters Vol. 17, No. 1, 85-89 (2016)

Preparation and characterization of chemically activated carbon materials for CO_2 capture

Da-Hee Jeon[1], Shin-Tae Bae[2] and Soo-Jin Park[1,♠]

[1]Department of Chemistry, Inha University, Incheon 22212, Korea
[2]Materials Development Center, Research & Development Division, Hyundai Motor Group, Hwaseong 18280, Korea

Key words: Activated carbons, CO_2 capture, KOH activation, Indoor CO_2 capture

Article Info

Received 3 July 2015
Accepted 20 December 2015

***Corresponding Author**
E-mail: sjpark@inha.ac.kr
Tel: +82-32-876-7234

Open Access

DOI: http://dx.doi.org/10.5714/CL.2016.17.1.085

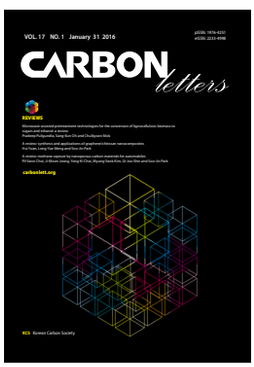

http://carbonlett.org

pISSN: 1976-4251
eISSN: 2233-4998

Atmospheric carbon dioxide (CO_2) exists as a gas at standard temperature and pressure, and it occurs in Earth's atmosphere in this state [1,2]. Rising levels of CO_2, a greenhouse gas, are a major environmental problem [3]. The main source of CO_2 emissions is the burning of fossil fuels, such as natural gas and coal. The combustion of these fossil fuels, such as natural gas, coal, and oil, is one of the major emission sources of CO_2 [4].

In addition to outdoor levels of CO_2, indoor levels of CO_2 have been extensively investigated because they have a direct impact on human health. Certain levels of CO_2 in indoor spaces cause symptoms such as headaches, vomiting, drowsiness, and dyspnea. Certain indoor spaces, such as automobiles, subways, and aircraft, have high concentrations of CO_2, which can cause serious health hazards. Thus, an increased CO2 concentration in these types of spaces is considered by many researchers to be a serious problem [5,6].

Recently, CO_2 capture and storage technology, including adsorption, absorption, cryogenics, and membranes, has received increased attention motivated by environmental concerns [7-9]. Absorption into an alkanolamine solution is a conventional and mature technology; however, this method has major drawbacks, such as high regeneration energy requirements and significant waste. However, adsorption using solid sorbents has attracted widespread interest over recent years because of its low energy consumption, lower regeneration requirements, and ease of conservation and recycling [10]. A wide range of solid adsorbents are currently under investigation, including zeolites, metal organic frameworks, porous carbon materials, macro-porous silica, and certain metal oxides [11-15]. Among the solid adsorbents for CO_2 capture, carbon materials, such as activated carbon (AC), carbon aerogels, graphene, and carbon nanotubes, have shown significant advantages because of their highly developed porosities and extended specific surface areas [16-24]. AC is of considerable interest because it is inexpensive, readily available, easily tuned, and thermally stable [25-27].

Surface modification can be performed *via* a range of treatments, such as chemical or electrochemical oxidation, chemical activation, and thermal treatment [28-30]. Chemical activation by $ZnCl_2$, NaOH, or KOH is an effective method of controlling the pore-size distributions and specific surface areas of carbon supports [31-35]. In particular, the chemical activation method using KOH has been the most widely studied. Researchers have reported that high specific surface areas and well-developed microporous structures can be obtained. Also, KOH activation is the most effective method in terms of the degree of activation.

In this study, we investigated the effects of KOH activation at various ratios on the surface of AC. Samples were prepared to evaluate highly efficient CO_2 capture capacities.

The KOH impregnation process was initiated by mixing 1 g of AC with 4 g of KOH in a water and ethanol solution (1:1). The resulting solution was stirred to ensure even mixing and vaporized for 48 h at 90°C. Then, the products were placed in a drying oven at 80°C overnight. The activation process was performed in a tube furnace under N_2 flow (200 mL/min); it involved heating the sample at a rate of 3 °C/min up to 900°C and maintaining this

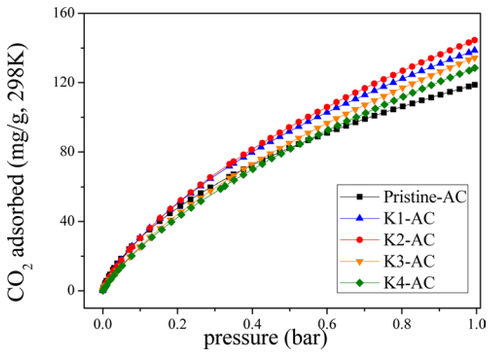

Fig. 1. N_2 full isotherms at 77 K porosity parameters of the Pristine-AC and K-AC samples

temperature for 1 h. The activated product was washed with a 2 M HCl solution and distilled water, filtered until it reached a pH of 7, and dried for 24 h at 80°C. The activated AC (i.e., KOH-AC) samples prepared at AC:KOH ratios of 0, 1:1, 1:2, 1:3, and 1:4 are here referred to as pristine-AC, K1-AC, K2-AC, K3-AC, and K4-AC, respectively.

The porous textures of the samples were determined from the N_2 adsorption-desorption isotherms at 77 K using a specific surface area and pore size analyzer (BELSORP, Osaka, Japan). Before the measurements, the prepared samples were outgassed at 200°C for 12 h under high vacuum through the degas port of the adsorption instruments. The Brunauer-Emmett-Teller (BET) equation was used to calculate the specific surface area, and the total pore volume (V_t) was obtained from the N_2 adsorption volume at $P/P_0 = 0.99$.

The samples were evaluated for their CO_2 capture capacities using the BELSORP instrument. The samples were degassed at 200°C for 12 h and cooled to the required adsorption temperature of 25°C. Then, the CO_2 adsorption volume was measured at a specific relative pressure (P/P_0) at 298 K.

The indoor CO_2 capture capacities of the samples were determined in a manufactured chamber at the laboratory scale. The initial concentration of CO_2 was about 400 ppm. The gas flow rate of CO_2 was adjusted using a flow controller. The atmosphere in the chamber was maintained with circulating CO_2 at a fixed flow rate of 8 mL/s for 10 min. During this process, the concentration of CO_2 was recorded every minute. The chamber

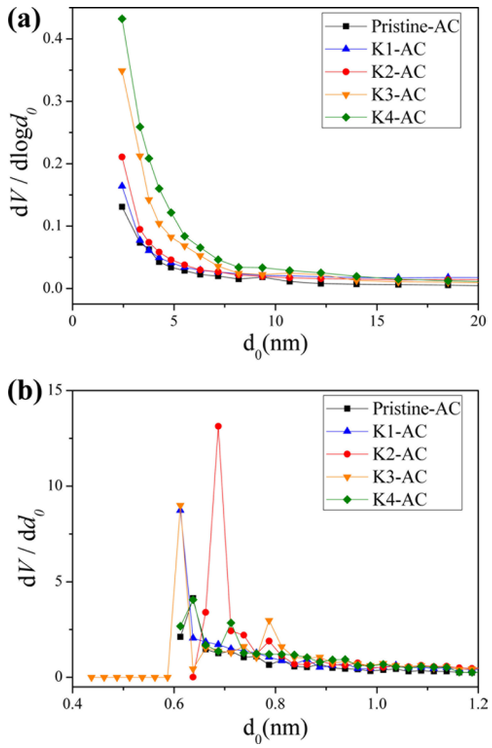

Fig. 2. Meso-(a) and micro-(b) pore size distribution of the Pristine-AC and K-AC samples

test was conducted using a CO_2 analyzer (IAQ8494; Tech one, Seoul, Korea).

N_2 adsorption/desorption isotherms and meso- and micropore size distribution curves were used to assess the textural surface properties of the prepared samples. From Fig. 1, it is evident that the prepared samples had Type I adsorption isotherms (IUPAC classification). Also, most of the pores had relative pressures below 0.1 as well as markedly increased adsorption amounts, indicating that these samples mainly consisted of well-developed micropores. As shown in Table 1, all prepared samples possessed BET surface areas of 800-1500 m^2/g. The total pore volumes and mesopore volumes tended to increase with increasing amounts of KOH up to the quantity in the K2-AC

Table 1. Textural properties of Pristine-AC and K-AC samples

Specimens	S_{BET} (m^2/g)[a]	V_{total} (cm^3/g)[b]	V_{meso} (cm^3/g)[c]	V_{micro} (cm^3/g)[d]	F_{micro} (%)[e]
Pristine-AC	898	0.394	0.053	0.341	86.5
K1-AC	1319	0.595	0.081	0.514	86.4
K2-AC	1507	0.670	0.090	0.580	86.5
K3-AC	1360	0.647	0.135	0.511	79.0
K4-AC	1227	0.615	0.171	0.443	72.0

[a] S_{BET} : specific surface area computed using BET equation ($P/P_0 = 0.05$-0.1).
[b] V_{total} : total pore volume ($P/P_0 = 0.990$).
[c] V_{meso} : micropore volume determined from the BJH equation.
[d] V_{micro} : mesopore volume determined from the subtraction of mesopore volume from total pore volume.
[e] F_{micro} : (micropore volume/total pore volume) × 100

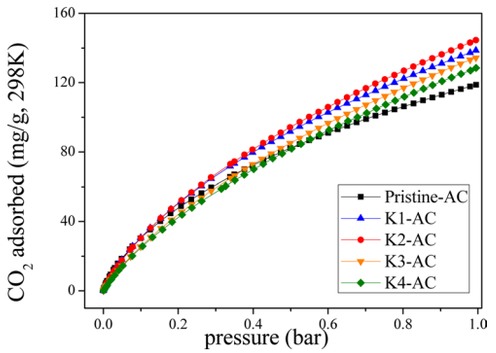

Fig. 3. CO_2 adsorption isotherms of the Pristine-AC and K-AC samples at 1 bar and 298 K.

sample. The K2-AC sample exhibited a large specific surface area (1507 m^2/g) and high total pore volume (0.670 cm^3/g) and micropore volume (0.580 cm^3/g). However, the surface areas, total pore volumes, and micropore volumes of the K3-AC and K4-AC samples were lower, likely because they contained excess KOH; large amounts of KOH destroyed the pore structures and increased the mesopore volumes.

As shown in Fig. 2a, the mesopore volume increased with increasing amounts of KOH. All samples had very sharp peaks at approximately 2 nm because they consisted mainly of micropores. As the amount of KOH increased, the mesopore volume rapidly increased. Fig. 2b shows the micropore size distribution of the pristine-AC and K-AC samples. Thus, micropores developed around pores with diameters between 0.6 and 0.8 nm, proving that they primarily developed in the parts of the prepared K-AC samples with pore diameters <1 nm.

Fig. 3 shows the CO_2 capture capacities of the pristine-AC and K-AC samples at 298 K and 1 bar. The CO_2 capture capacity of pristine-AC was 118.75 mg/g, while the K2-AC sample had the highest CO_2 capture capacity of 144.5 mg/g at 298 K and 1 atm. The CO_2 capture capacities of the samples decreased in the following order: K2-AC > K1-AC > K3-AC > K4-AC > pristine-AC, as shown in Fig. 3. The improvement of the CO_2 capture capacities resulted from the development of micropores and increased specific surface areas. However, in the cases of K3-AC and K4-AC, the CO_2 capture capacities were reduced because of the destruction of the pore structures by excess KOH. Therefore, the amount of KOH significantly affected the CO_2 capture capacity. Chemical activation using KOH increased the CO_2 capture capacity by controlling the meso- and micro-pore volumes and specific surface areas.

Fig. 4 shows the indoor CO_2 capture capacities of the pristine-AC and K-AC samples, as determined using the chamber test. The chamber test was conducted in a manufactured chamber at the laboratory scale. Fig. 4a shows that the initial CO_2 concentration of each sample test was about 400 ppm. The atmosphere in the chamber was maintained with circulating CO_2 at a fixed flow rate of 8 mL/s for 10 min using a flow controller. After 10 min, the CO_2 concentration of the non-adsorbents, i.e., pristine-AC, and the prepared samples, i.e., K1-AC, K2-AC, K3-AC, and K4-AC, were 4060, 3459, 3020, 2756, 3140, and 3445 ppm, respectively. As expected, the adsorbents made a significant difference, with a maximum concentration reduction of 1304 ppm.

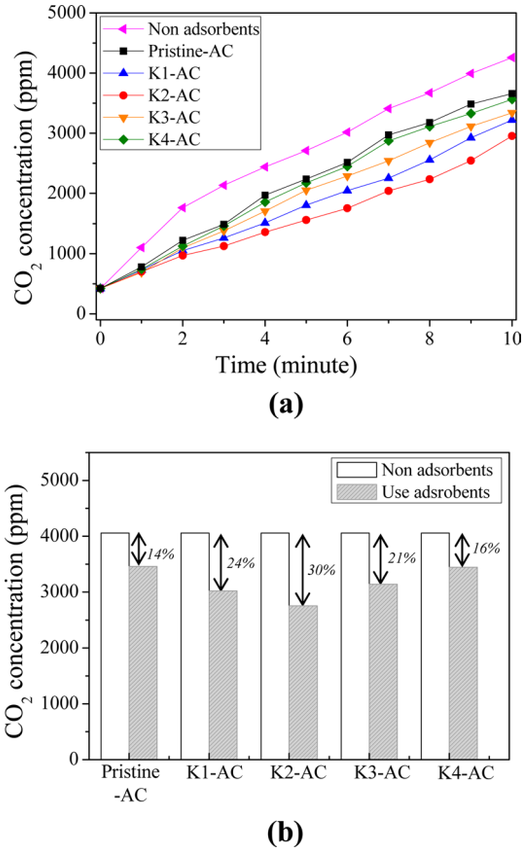

Fig. 4. Indoor CO_2 capture capacity of the Pristine-AC and K-AC samples.

Fig. 4b presents the same results as Fig. 4a; however, Fig. 4b shows them as percentages of the indoor CO_2 capture capacity. The indoor CO_2 capture capacity rates decreased in the following order: K2-AC > K1-AC > K3-AC > K4-AC > pristine-AC. Therefore, the amount of KOH affected the indoor CO_2 capture capacity rate. K2-AC featured the highest indoor CO_2 capture capacity rate of approximately 30%, because of its well-developed micropore size (approximately 0.68 nm) with an appropriate amount of KOH. It can be concluded that pore size of 0.68 nm may the optimal value for indoor CO_2 capture. In contrast, K4-AC had a significantly lower indoor CO_2 capture capacity rate of 16%, which was the same as that of pristine-AC. An appropriate amount of KOH improved the indoor CO_2 capture capacity rate; however, excess KOH resulted in the destruction of the pore structures.

We investigated the effects of activation using various amounts of KOH on the surface of AC. The K2-AC sample exhibited a large specific surface area (1507 m^2/g) and high total pore volume (0.670 cm^3/g) and micropore volume (0.580 cm^3/g). The micropores in the K-AC samples appeared primarily in parts where the pore diameters were < 1 nm.

One of the prepared K-AC samples, namely, K2-AC, exhibited a high CO_2 capture capacity of 144.5 mg/g and an indoor CO_2 capture capacity rate of about 30%. The excellent CO_2 capture capacity and high indoor CO_2 capture capacity rate were attributed to the optimized amount of KOH.

Conflict of Interest

No potential conflict of interest relevant to this article was reported.

Acknowledgments

This work was supported by the Hyundai NGV (Technology Research Team) and Hyundai Motor Group (Eco Technology Research Team).

References

[1] Lastoskie C. Caging carbon dioxide. Science, **330**, 595 (2010). http://dx.doi.org/10.1126/science.1198066.

[2] Keith DW. Why capture CO_2 from the atmosphere? Science, **325**, 1654 (2009). http://dx.doi.org/10.1126/science.1175680.

[3] Chaffee AL, Knowles GP, Liang Z, Zhany J, Xiao P, Webley PA. CO_2 capture by adsorption: materials and process development. Int J Greenhouse Gas Control, **1**, 11 (2007). http://dx.doi.org/10.1016/S1750-5836(07)00031-X.

[4] Jacobson MZ. Review of solutions to global warming, air pollution, and energy security. Energy Environ Sci, **2**, 148 (2009). http://dx.doi.org/10.1039/b809990c.

[5] Zhao J, Yang X. Photocatalytic oxidation for indoor air purification: a literature review. Build Environ, **38**, 645 (2003). http://dx.doi.org/10.1016/S0360-1323(02)00212-3.

[6] Daisey JM, Angell WJ, Apte MG. Indoor air quality, ventilation and health symptoms in schools: an analysis of existing information. Indoor Air, **13**, 53 (2003). http://dx.doi.org/10.1034/j.1600-0668.2003.00153.x.

[7] Li JR, Ma Y, McCarthy MC, Sculley J, Yu J, Jeong HK, Balbuena PB, Zhou HC. Carbon dioxide capture-related gas adsorption and separation in metal-organic frameworks. Coord Chem Rev, **255**, 1791 (2011). http://dx.doi.org/10.1016/j.ccr.2011.02.012.

[8] Meng LY, Park SJ. Effect of exfoliation temperature on carbon dioxide capture of graphene nanoplates. J Colloid Interface Sci, **386**, 285 (2012). http://dx.doi.org/10.1016/j.jcis.2012.07.025.

[9] Rao AB, Rubin ES. A technical, economic, and environmental assessment of amine-based CO_2 capture technology for power plant greenhouse gas control. Environ Sci Technol, **36**, 4467 (2002). http://dx.doi.org/10.1021/es0158861.

[10] Bae YS, Snurr RQ. Development and evaluation of porous materials for carbon dioxide separation and capture. Angew Chem Int Edit, **50**, 11586 (2011). http://dx.doi.org/10.1002/anie.201101891.

[11] Banerjee R, Phan A, Wang B, Knobler C, Furukawa H, O'Keeffe M, Yaghi OM. High-throughput synthesis of zeolitic imidazolate frameworks and application to CO_2 capture. Science, **319**, 939 (2008). http://dx.doi.org/10.1126/science.1152516.

[12] Simmons JM, Wu H, Zhou W, Yildirim T. Carbon capture in metal-organic frameworks-a comparative study. Energy Environ Sci, **4**, 2177 (2011). http://dx.doi.org/10.1039/c0ee00700e.

[13] Park SJ, Kim KD. Adsorption behaviors of CO_2 and NH_3 on chemically surface-treated activated carbons. J Colloid Interface Sci, **212**, 186 (1999). http://dx.doi.org/10.1006/jcis.1998.6058.

[14] Lee SY, Park SJ. Determination of the optimal pore size for improved CO_2 adsorption in activated carbon fibers. J Colloid Interface Sci, **389**, 230 (2013). http://dx.doi.org/10.1016/j.jcis.2012.09.018.

[15] Hughes RW, Lu DY, Anthony EJ, Macchi A. Design, process simulation and construction of an atmospheric dual fluidized bed combustion system for in situ CO_2 capture using high-temperature sorbents. Fuel Process Technol, **86**, 1523 (2005). http://dx.doi.org/10.1016/j.fuproc.2005.01.006.

[16] Meng LY, Park SJ. Effect of heat treatment on CO_2 adsorption of KOH-activated graphite nanofibers. J Colloid Interface Sci, **352**, 498 (2010). http://dx.doi.org/10.1016/j.jcis.2010.08.048.

[17] Meng LY, Park SJ. Superhydrophobic carbon-based materials: a review of synthesis, structure, and applications. Carbon Lett, **15**, 89 (2014). http://dx.doi.org/10.5714/CL.2014.15.2.089.

[18] Meng LY, Park SJ. Effect of nano-silica spheres template on CO_2 capture of exchange resin-based nanoporous carbons. J Nanosci Nanotechnol, **13**, 401 (2013). http://dx.doi.org/10.1166/jnn.2013.6931.

[19] Park SJ, Jang YS, Shim JW, Ryu SK. Studies on pore structures and surface functional groups of pitch-based activated carbon fibers. J Colloid Interface Sci, **260**, 259 (2003). http://dx.doi.org/10.1016/S0021-9797(02)00081-4.

[20] Presser V, McDonough J, Yeon SH, Gogotsi Y. Effect of pore size on carbon dioxide sorption by carbide derived carbon. Energ Environ Sci, **4**, 3059 (2011). http://dx.doi.org/10.1039/c1ee01176f.

[21] Yoo HM, Lee SY, Park SJ. Ordered nanoporous carbon for increasing CO_2 capture. J Solid State Chem, **197**, 361 (2013). http://dx.doi.org/10.1016/j.jssc.2012.08.035.

[22] Garcia-Gallastegui A, Iruretagoyena D, Gouvea V, Mokhtar M, Asiri AM, Basahel SN, Al-Thabaiti SA, Alyoubi AO, Chadwick D, Shaffer MSP. Graphene oxide as support for layered double hydroxides: enhancing the CO_2 adsorption capacity. Chem Mater, **24**, 4531 (2012). http://dx.doi.org/10.1021/cm3018264.

[23] Siriwardane RV, Shen MS, Fisher EP, Poston JA. Adsorption of CO_2 on molecular sieves and activated carbon. Energy Fuels, **15**, 279 (2001). http://dx.doi.org/10.1021/ef000241s.

[24] Kim BJ, Lee YS, Park SJ. Novel porous carbons synthesized from polymeric precursors for hydrogen storage. Int J Hydrogen Energ, **33**, 2254 (2008). http://dx.doi.org/10.1016/j.ijhydene.2008.02.019.

[25] Im JS, Park SJ, Lee YS. Preparation and characteristics of electrospun activated carbon materials having meso- and macropores. J Colloid Interface Sci, **314**, 32 (2007). http://dx.doi.org/10.1016/j.jcis.2007.05.033.

[26] Park SJ, Jang YS. Pore structure and surface properties of chemically modified activated carbons for adsorption mechanism and rate of Cr(VI). J Colloid Interface Sci, **249**, 458 (2002). http://dx.doi.org/10.1006/jcis.2002.8269.

[27] Park SJ, Jin SY. Effect of ozone treatment on ammonia removal of activated carbons. J Colloid Interface Sci, **286**, 417 (2005). http://dx.doi.org/10.1016/j.jcis.2005.01.043.

[28] Frackowiak E, Béguin F. Carbon materials for the electrochemical storage of energy in capacitors. Carbon, **39**, 937 (2001). http://dx.doi.org/10.1016/S0008-6223(00)00183-4.

[29] Ahmadpour A, Do DD. The preparation of active carbons from coal by chemical and physical activation. Carbon, **34**, 471 (1996). http://dx.doi.org/10.1016/0008-6223(95)00204-9.

[30] Martín-Jimeno FJ, Suárez-García F, Paredes JI, Martínez-Alonso A, Tascón JMD. Activated carbon xerogels with a cellular morphology derived from hydrothermally carbonized glucose-gra-

phene oxide hybrids and their performance towards CO_2 and dye adsorption. Carbon, **81**, 137 (2015). http://dx.doi.org/10.1016/j.carbon.2014.09.042.

[31] Hayashi J, Kazehaya A, Muroyama K, Watkinson AP. Preparation of activated carbon from lignin by chemical activation. Carbon, **38**, 1873 (2000). http://dx.doi.org/10.1016/S0008-6223(00)00027-0.

[32] Mohammadi SZ, Hamidian H, Moeinadini Z. High surface area-activated carbon from Glycyrrhiza glabra residue by $ZnCl_2$ activation for removal of Pb(II) and Ni(II) from water samples. J Ind Eng Chem, **20**, 4112 (2014). http://dx.doi.org/10.1016/j.jiec.2014.01.009.

[33] Martins AC, Pezoti O, Cazetta AL, Bedin KC, Yamazaki DAS, Bandoch GFG, Asefa T, Visentainer JV, Almeida VC. Removal of tetracycline by NaOH-activated carbon produced from macadamia nut shells: kinetic and equilibrium studies. Chem Eng J, **260**, 291 (2015). http://dx.doi.org/10.1016/j.cej.2014.09.017.

[34] Lillo-Ródenas MA, Cazorla-Amorós D, Linares-Solano A. Understanding chemical reactions between carbons and NaOH and KOH: an insight into the chemical activation mechanism. Carbon, **41**, 267 (2003). http://dx.doi.org/10.1016/s0008-6223(02)00279-8.

[35] Jung MJ, Jeong E, Kim Y, Lee YS. Influence of the textual properties of activated carbon nanofibers on the performance of electric double-layer capacitors. J Ind Eng Chem, **19**, 1315 (2013). http://dx.doi.org/10.1016/j.jiec.2012.12.034.